Draft version -0.1

ATLAS NOTE

ATL-PHYS-INT-2008-0xy

May 6, 2008

Cross sections for Standard Model processes to be used in the ATLAS CSC notes

The ATLAS Cross Section Task Force
Editors:
Daniela Rebuzzi, Markus Schumacher
Contributors:
Shoji Asai, Clement Benoit, Maarten Boonekamp, Craig Buttar,
Jon Butterworth, Dave Charlton, Tiesheng Dai, Martine Fernandez-Bosman,
Pamela Ferrari, Martijn Gosselink, Ian Hinchliffe, Sandra Horvat, Joey Huston, Karl Jakobs,
Osamu Jinnouchi, Borut Kersevan, Thomas Le Compte, Wolfgang Mader,
Bruce Mellado, Arthur Moraes, Marek Schoenherr, Akira Shibata,
Maria Smizanska, Markus Warsinsky, Seth Zenz, Bing Zhou

Abstract

This paper summarises the cross sections for Standard Model processes to be used in evaluation of the ATLAS physics potential during the CSC effort. Recommendations will be given on how to normalise event samples generated with various Monte Carlo generators.

1 Introduction

A common use of cross sections for various processes in all ATLAS Monte Carlo studies is of importance in order to derive a consistent picture of the physics potential of the ATLAS experiment. This paper summarizes the cross sections for Standard Model processes to be used in evaluation of the physics potential during the Computing System Commissioning (CSC) effort. Recommendations will be given on how to normalize event samples generated with various Monte Carlo generators.

The CTEQ6L1 and CTEQ6M parton density functions [1–4] have been used for the calculation of the cross sections at leading order (LO) and next-to-leading order (NLO) in perturbation theory, respectively. The uncertainties arising from the choice of the renormalisation and factorisation scales have been estimated by decreasing and increasing the central scale values to one half and two the energy scale of the process, respectively. Exceptions to the above statements are explicitly mentioned in the text. One should note that for most of the processes discussed below no NLO event generators exist yet.

The events are generated with LO programs which in several cases use a matching scheme between matrix element calculation and parton shower simulation. Hence one should be aware that the normalisation of those event samples especially with large jet multiplicities to (N)NLO cross sections might not yield the correct description when requiring large jet multiplicities in the event selection. This is of particular importance if very specific regions of the phase space are selected in the analysis. The individual analysis should make sure that the event generation and cross section normalisation is appropriate for the selection applied.

The numbers reported in this note take only into account higher order corrections due to strong interaction as described by quantumchromo dynamics (QCD). Electroweak corrections are also sizable for several processes discussed below and in some cases larger than the uncertainties from missing higher order QCD corrections. However, a consistent evaluation of these correction and their inclusion is beyond the scope of this compilation.

2 Production of a single electroweak gauge boson

2.1 W and Z production

ATLAS uses several physics generators for the simulation of W and Z production. Two of them, PYTHIA [5] and HERWIG [6–8], are Leading Order (LO) matrix element generators. Although the normalisation is LO, the description of the observable distributions is refined through the application of soft emission resummation (or parton shower), providing a realistic description of the W and Z p_T distributions in the low p_T region.

A further improvement lies in the coherent merging of the parton shower with an $O(\alpha_S)$ matrix element correction at higher p_T, providing a Leading Order description of $d\sigma/dp_T$ in this range. Another approach is to match the LO matrix elements for various additional parton multiplicities with the parton shower in order to obtain a good description at low and large transverse momentum of the produced gauge boson. This method of matching is implemented in the ALPGEN [9–11] and SHERPA [12, 13] MC generators with different schemes for the matching.

Recently, the new MC cross section integrator FEWZ became available [14, 15]. The LO, NLO and NNLO cross section for W and Z production can be computed including cuts on the decay leptons phase space. In principle, this gives the possibility to produce fully differential distributions to NNLO precision. However, no consistent resummation procedure exists at NNLO, and as result the W and Z p_T distributions are unphysical at low p_T and hence are not shown in the following. In addition, very long calculation times*) prevents the accurate computation of distributions. Nevertheless, the inclusive

*) NNLO calculation for the inclusive cross section takes about 24h on a 2GHz computer.

cross section calculation has a theoretical uncertainty, as estimated from the renormalization scale dependance of the results, well below 1%. This remarkable result opens the way for high precision physics at the LHC, enabling precise proton PDF determination through W and Z production, improved machine luminosity determination from the counting of these processes, with implications on all LHC physics.

The results of the cross section calculations obtained from FEWZ are shown in Table 1. This cross sections include the branching ratio into one charged lepton family according to the values obtained by the particle data group. The factorisation and renormalisation scale have been set to the boson mass under consideration. The uncertainties implied by our approach are briefly discussed below.

Table 1: LO, NLO and NNLO values for inclusive cross sections for W and Z production with subsequent decay into $W \to \ell\nu$ and $Z \to \ell^+\ell^-$, respectively. The values quoted are given in pb and correspond to one lepton genaration. They have been calculated with the MC program FEWZ.

process	PDF	LO	NLO	NLO
W^+	MRST01	9963	12032	11755
W^+	CTEQ6.1	9732	11910	11825
W^-	MRST01	7338	8938	8701
W^-	CTEQ6.1	7099	8764	8685
Z (60 GeV $< M_{\ell^+\ell^-}$)	MRST01	1715	2083	2036
Z (50 GeV $< M_{\ell^+\ell^-} <$ 500 GeV)	MRST01	1764	2137	2064
Z (60 GeV $< M_{\ell^+\ell^-}$)	CTEQ6.1	1656	2032	2015
Z (50 GeV $< M_{\ell^+\ell^-} <$ 500 GeV)	CTEQ6.1	1704	2087	2052

Firstly, the remaining scale dependence is found in [14, 15] to be smaller than 1%. Secondly, the Monte Carlo integration method used by the program provides, within reasonable running time, a statistical accuracy of about 2% on the total cross section. The uncertainty from variation of the parton distribution function have been found to correspond to 8%.

The lepton distributions are also affected by the higher order corrections. Hence, the acceptance of cuts applied on LO distributions carries some uncertainty. It was found (see also [14,15]) that for typical fiducial cuts ($|\eta| < 2.5$, $p_T > 20$ GeV) the acceptance as predicted from LO generators differs by up to 2% from the NNLO result.

Let us finally quote a recent update of the CTEQ PDF analysis. In [3] heavy quark mass terms were properly incorporated in the formalism, leading to an increase of the W and Z cross sections by about 8%. Having produced our samples with the CTEQ6.1 sets well before these results appeared, we reserve the study of these effects for future work.

The leading order cross sections for PYTHIA and HERWIG event samples should be renormalised to reproduce the NNLO numbers for the cross section times branching ratio quoted in Tab.1. For the production of a Z boson the number corresponding to the phase space $M_{\ell^+\ell^-} > 60$ GeV should be applied. The cross section at LO obtained with ALPGEN for the $W + jets$ sample, after the matching between parton shower and matrix elements has been performed, corresponds to 17 794 pb including a branching ratio of 11.11% for leptonic decays of the W boson. In order to normalise to the recommended inclusive cross section value from FEWZ the cross sections from ALPGEN should be multiplied by a factor of 1.15. The cross section at LO obtained from ALPGEN for $Z + jets$ sample, after the matching between parton shower and matrix element has been performed, corresponds to 9602 pb for the $Z \to \nu\nu$ decay mode and to 1649 pb for the $Z \to \ell^+\ell^-$ decay mode. This numbers include a branching ratio for $Z \to \nu\nu$ of 20.35% and for $Z \to \ell^+\ell^-$ of 3.43% in ALPGEN and corresponds to a phase space of $50 < M_{\ell^+\ell^-} < 500$ GeV. Neglecting the very small contribution from photon exchange a normalisation factor of 1.24 for the ALPGEN $Z + jet$ samples has been derived.

A detailed study investigated the dependence of the cross section for gauge boson plus at least four additional jets with transverse momentum above 20 GeV in ALPGEN on the matching parameters used in the event generation. It was found that the accepted cross sections vary by a factor of two. For lower jet multiplicties the uncertainty will most probably be smaller but no explicit number was derived. It is forseen to measure those cross sections with signifanctly better accuracy from the first data collected at the LHC.

The LO value for QCD induced production of weak gauge bosons plus jets obtained by SHERPA [12, 13] are summarised in Table 2. The branching ratios used in SHERPA are: BR($Z \to \nu\nu$) = 6.7%,

Table 2: LO cross sections calculated with SHERPA for single production of a massive weak gauge boson. The values are given in pb and include the branching ratio into one lepton family.

process	cross section
$W \to \ell\nu$ (1 GeV $< M_{\ell\nu}$)	15686
$Z \to \ell^+\ell^-$ (60 GeV $< M_{\ell^+\ell^-}$)	1472
$Z \to \nu\nu$ (1 GeV $< M_{\nu\nu}$)	8616

BR($Z \to \ell^+\ell^-$) = 3.5% and BR($W \to \ell\nu$) = 10.0%. From this numbers we derive a normalisation factor of 1.32 for the $W + jets$ samples and 1.37 for the $Z + jets$ samples.

A comparison of the distribution of the transverse momentum of the gauge bosons for various MC generators and the cross section calculator RESBOS [16–18], which includes a NLO calculation plus NLL (next-to-leading log) resummation of QCD effects at low transverse momentum, is shown in Figures 1 and 2. As expected the different approaches for event generation agree at large transverse momentum, however signifcant differences are observed for transverse momenta below ≈ 50 GeV.

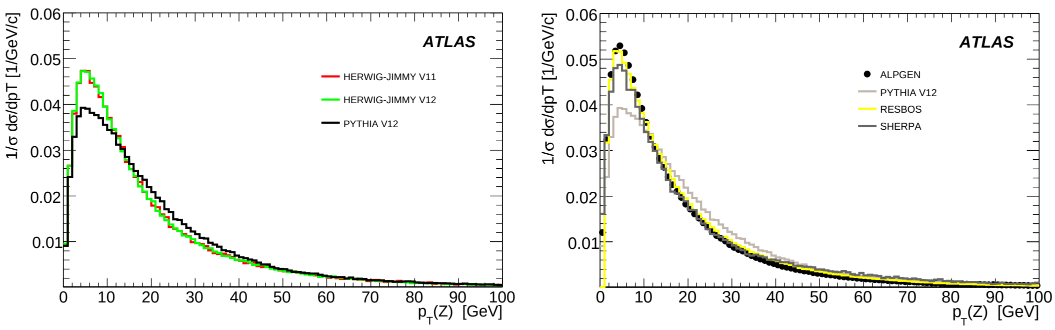

Figure 1: The transverse momentum spectrum of the Z from various MC generators. All distributions are normalised to unity.

2.2 Production of a photon in association with jets

The total inclusive cross section for the γj process was obtained using the package JETPHOX [19]. This package computes the direct and fragmentation single photon production. The distribution of the photon p_T obtained with this package was compared with that obtained for the direct production using PYTHIA. It was observed that the differential cross section obtained with JETPHOX was a factor of 2.1 larger than that obtained with PYTHIA, with a weak p_T dependence. When a $p_{T\gamma} > 25$ GeV cut is

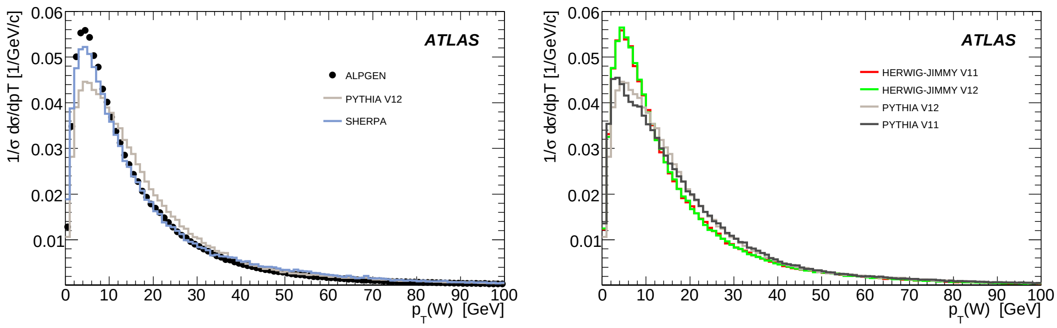

Figure 2: The transverse momentum spectrum of the W from various MC generators. All distributions are normalised to unity.

applied, the cross section results:

$$\sigma_{\gamma jet} = 180 \times 10^3 \text{pb}.$$

The total γj cross section evaluated with ALPGEN agrees at the level of 10% with the result above, after the application of the corresponding cuts.

3 Production of a pair of electroweak weak gauge bosons

3.1 ZZ production

The LO pair productions of Z bosons receives contributions to order α^2 from $q\bar{q}$ initiated and to order $\alpha^2\alpha_s^2$ via a box diagram from gg initiated processes. The $q\bar{q} \to Z(\gamma)Z(\gamma)$ contributions, up to NLO, can be calculated with MCFM [19]. When a $M_{Z/\gamma} >$12 GeV cut is set, corresponding to the default cuts when using PYTHIA for event generation, the LO and NLO cross sections, without taking into account any branching ratios correspond to

$$\sigma_{LO} = 16.489 \pm 0.046 \text{ (stat) pb and}$$
$$\sigma_{NLO} = 22.058^{+0.1}_{-0.2}(\mu_R = \mu_F) \pm 0.714 \text{ (PDF) } \pm 0.037. \text{ (stat) pb}$$

From the numbers above, a k-factor of 1.34 is derived. The LO cross section value evaluated with PYTHIA, including the sum of branching ratios into electrons, muons and taus corresponds to 159.00 $\pm$ 0.05 fb. PYTHIA correctly takes into account the different couplings of photon and Z to leptons in the final state whereas MCFM uses Z branching ratios also for the photon contribution. Hence we recommend to use the PYTHIA prediction scaled by the k-factor obtained from MCFM[†)]. The *effective* cross section, with subsequent decays in electron, muons or tau leptons, for ZZ samples produced with PYTHIA is therefore:

$$\sigma_{Z(\gamma)Z(\gamma)} = 159 \text{ fb} \times [k = 1.34 + 0.3(gg)] = 261 \text{ fb}.$$

The 0.3 term accounts for the box contribution from gg induced Z pair production. A more correct evaluation would require to use the MC event generator GG2ZZ [20] which implements the gluon induced contribution instead of simply increasing the LO value by 30%. The estimate for the uncertainty on

[†)] It has been checked that the LO values for undecayed Z bosons agree on the 5% level between PYTHIA and MCFM.

Table 3: K-factors for the ZZ background (for $M_{Z/Z^*} > 12$ GeV). The error on the K-factors is dominated by the systematics (from PDF and renormalization and factorization scales) and amounts to 3.3%.

M_{ZZ} (GeV)	K-factor
[115,125]	1.15
[125,135]	1.21
[145,155]	1.25
[155,165]	1.34
[175,185]	1.31
[195,205]	1.32
[295,305]	1.40
[395,405]	1.52

the NLO cross section receives a contribution of ∼3% from the PDFs and of ∼1% from the QCD scale choice. The central value for the renormalisation and factorisation scales is the average mass of the Z bosons ‡)). It should be noted that the k-factor depends on the invariant diboson mass, and spans in the range from 1.15 to 1.52 for $Z(\gamma)Z(\gamma)$ masses between 120 and 4s00 GeV as in Table 3.1. Analyses sensitive to this mass distribution should take into account this fact.

When HERWIG is used to generate ZZ events (always through the $q\bar{q} \to Z(\gamma)Z(\gamma)$ contribution), an internal cut on the boson masses is applied at 20 GeV. The LO and NLO values, calculated with MCFM for $M_{Z/\gamma}$ >20 GeV and for $p_T(Z) > 10$ GeV, amount to

$$\sigma_{LO} = 13.76 \pm 0.01 \text{ (stat) pb and}$$
$$\sigma_{NLO} = 17.8^{+0.1}_{-0.4}(\mu_R = \mu_F) \pm 0.745 \text{ (PDF) } \pm 0.1 \text{ (stat) pb.}$$

The LO cross section for the quark initiated process from MCFM agrees with the LO evaluation from HERWIG only at a level of 20%, when the same phase space cuts are applied, and this should be investigated. The recommendation for HERWIG ZZ sample is to normalize to the MCFM NLO cross section above. To account for the gluon initiated process one should also scale the LO cross section by 30% or, preferably, generate separately events with GG2ZZ.

MC@NLOis also used to generate ZZ samples. As already mentioned, it provides NLO event generation, incorporating NLO QCD matrix elements consistently into HERWIG parton shower framework. A comparison of the NLO values obtained with MC@NLO and MCFM for weak gauge boson masses larger than 75 GeV shows agreement at the 3% level.

3.2 *WW* production

The pair productions of W bosons receives contributions at order α^2 from $q\bar{q}$ initiated and at order $\alpha^2\alpha_s^2$ via a box diagram from gg initiated processes.

The contribution from $gg \to W^+W^- \to e^+\nu_e\mu^-\bar{\nu}_\mu$ proceeding via a box diagram has been evaluated to be 60.00 fb as calculated with the event generator GG2WW using the CTEQ6M parton density functions.

The contribution for $q\bar{q} \to W^+W^-$ has been calculated up to NLO with MCFM for various restrictions of the phase space corresponding to the default cuts used in the event generation with HERWIG and PYTHIA. They are listed in Table 4 (not including W branching ratios). The QCD scale uncertainty on the NLO cross sections corresponds to 2% while the PDF uncertainty amounts to 3%. The recommendation is to use the NLO value from the table above corresponding to the phase space generated in the

‡) Setting the scales to $M^2(Z) + p_T^2(Z)$ does not produce any appreciable variation to the inclusive cross section.

Table 4: NLO cross sections for $q\bar{q} \to WW$ as obtained with MCFM.

phase space	cross section (pb)	k-factor
M_W >12 GeV	112.5 ± 0.2	1.57
M_W >20 GeV	112.4 ± 0.2	1.56
M_W >30 GeV	112.2 ± 0.2	1.56
M_W >75 GeV	101.5 ± 0.2	1.56
M_W >20 GeV, p_T^W >10 GeV	112.43 ± 0.06	1.57

MC event sample under consideration for the quark initiated process. For the gluon initiated process one may either scale the cross section in order to take into account this contribution or preferably generate separately events with GG2WW.

The LO cross sections for the quark initiated process from MCFM have been found to agree with the LO values as obtained from HERWIG on a level of better than 3%. For instance, with the cuts of the last row (M_W >20 GeV, p_T^W >10 GeV), the LO cross section from HERWIG results 70 pb, while MCFM provides $\sigma_{LO} = 71.69 \pm 0.04$ (stat) pb. The residual difference can be attributed to different schemes for evaluation the EW parameters, different scale choices and different branching ratios implemented in the two programs.

The NLO value obtained from MC@NLO agrees also with the value from MCFM on the level of 2%, when the same cuts on the phase space are applied. For instance, when (M_W >20 GeV, p_T^W >10 GeV), MCFM provides $\sigma_{NLO} = 112.43^{+2.5}_{-1.4}(\mu_R = \mu_F) \pm XXX$ (PDF) ± 0.06 (stat) pb, while MC@NLO gives $\sigma_{NLO} = 110.46$ pb.

3.3 WZ production

Pair production of a W and aZ bosons are know only in terms of the $q\bar{q} \to WZ$ contribution, which is implemented both in HERWIG and in PYTHIA. The NLO cross section obtained with MCFM for $M_{W/Z} > 20$ GeV and $p_T^{W/Z} > 10$ GeV amounts to:

$$\sigma_{W^+Z} = 34.752^{+1.2}_{-0.9}(\mu_R = \mu_F) \pm 1.043 \text{ (PDF) } \pm 0.004 \text{ (stat) pb}$$
$$\sigma_{W^-Z} = 21.684^{+0.5}_{-0.9}(\mu_R = \mu_F) \pm 0.905 \text{ (PDF) } \pm 0.003 \text{ (stat) pb}$$

for the two differently charged W , which give rise to a total cross section $\sigma_{NLO} = 56.43$ pb with a maximum uncertainty of 3% due to the QCD scale variation and 3% uncertainty due to the PDFs. We recommend to normalize to this NLO cross section.

The LO cross sections evaluated with MCFM corresponds to 31.75 ± 0.01 pb, adding the W^-Z and W^+Z contributions, giving rise to a k-factor = 1.78 ± 0.01. The LO MCFM prediction is in good agreement with LO MC event generator cross sections, as well as the NLO prediction with respect to MC@NLO results.

3.4 $\gamma\gamma$ production

Diphoton production proceeds via two sets of diagrams, $q\bar{q}, qg \to \gamma\gamma$ to order $\alpha^2\alpha_s$ (usually referred to the Born and Bremsstrahlung contributions) and $gg \to \gamma\gamma$ to order $\alpha^2\alpha_s^3$ (usually refereed to as the Box contribution). Contributions from photons produced collinear to quarks are also taken into account at NLO. DIPHOX [21] and RESBOS [16–18] are used for the generation of the $\gamma\gamma$ process. DIPHOX includes all the processes to order $\alpha^2\alpha_s$, including Bremsstrahlung contributions with the quasi collinear fragmentation of quarks and gluons, which are computed at NLO. It does not include resummation effects. RESBOS includes Born and Box at NLO as well as the bremsstrahlung contribution (but the fragmentation contribution is only evaluated at LO). RESBOS includes resummation effects to NNLL. In these computations, a parton level isolation cut of 10 GeV on the energy deposited in a cone of 0.4 is used. This was checked against the real photon identification cuts using PYTHIA fully simulated events and an overall k-factor = 2.1 has been estimated against the LO PYTHIA prediction. DIPHOX and RESBOS predictions for the total irreducible background agree to better than 10% [22].

We recommend to use the following cross section for diphoton production:

$$\text{Born and Brems} \quad q\bar{q}, qg \to \gamma\gamma : \sigma = 20.87\,\text{pb and}$$
$$\text{Box} \quad gg \to \gamma\gamma : \sigma = 7.98\,\text{pb}.$$

The values have been calcuated with RESBOS for $80 < M_{\gamma\gamma} < 150$ GeV, where $M_{\gamma\gamma}$ is the invariant mass of the di-photon system, and $p_{T\gamma} > 25$ GeV, where $p_{T\gamma}$ is the transverse momentum of the photons. Photons were required to lie in the central detector region, $|\eta| < 2.5$. The factorisation and renormalisation scales were set dynamically to the invariant mass of the di-photon system. By varying them from 0.5 $\times M_{\gamma\gamma}$ to 2 $\times M_{\gamma\gamma}$, an overall variation of 3% on the total cross section is observed. The uncertainties related to parton distribution functions are of the order of 10%, while uncertainties due to multi parton contributions can amount to 18%. The total systematic uncertainties on the effective cross sections, including all the possible contributions, can be estimated equal to $\sim$22%.

4 Production of top quarks

4.1 Pairproduction of top quarks

Several calculations beyond LO have been performed. At NLO a cross section of 794 ± 32 pb has been derived which increases to 872.8 ± 15 pb when NNLL soft-gluon corrections are included [23]. We recommend to use the value at NLO including NLL resummation of soft effects [24] of:

$$\sigma_{t\bar{t}} = 833\,\text{pb}.$$

The uncertainties due to missing higher order corrections and due to uncertainties in the parton density functions have been estimated to be 100 pb.

The cross sections obtained from MC@NLO is 774 pb. Hence the cross sections of the event samples generated with MC@NLO should be corrected by the factor 833/774. Additional samples with multiple jets in the final state arising from matrix element calculations have been generated using ALPGEN with the MLM matching procedure. The LO cross sections for the ALPGEN samples after MLM matching correspond to 414 (404) pb for a matching scales of 20 (40) GeV. Hence we recommend to scale the cross sections to be used for the ALPGEN event samples by 2.01 for a matching scale of 20 GeV and 2.06 for a matching scale of 40 GeV. Those factors do not include a correction for the branching ratios which are different in ALPGEN by default with respect to the particle data group values. The values used in ALPGEN for $W \to \ell\nu$ is 1/9. The individual analyses should correct for this. The transverse momentum distributions for the top quark pair and the individual top quarks for three different MC genearors are shown in Figures 3 and 4.

4.2 Production of a single top quark

For single top production three production mechanisms are distinguished: (i) s-channel, (ii) t-channel and (iii) Wt production. ACERMC [25] is used for the event generation which also provides the LO cross section values shown in the table below summed for t and $\bar{t}$ production not including any decay

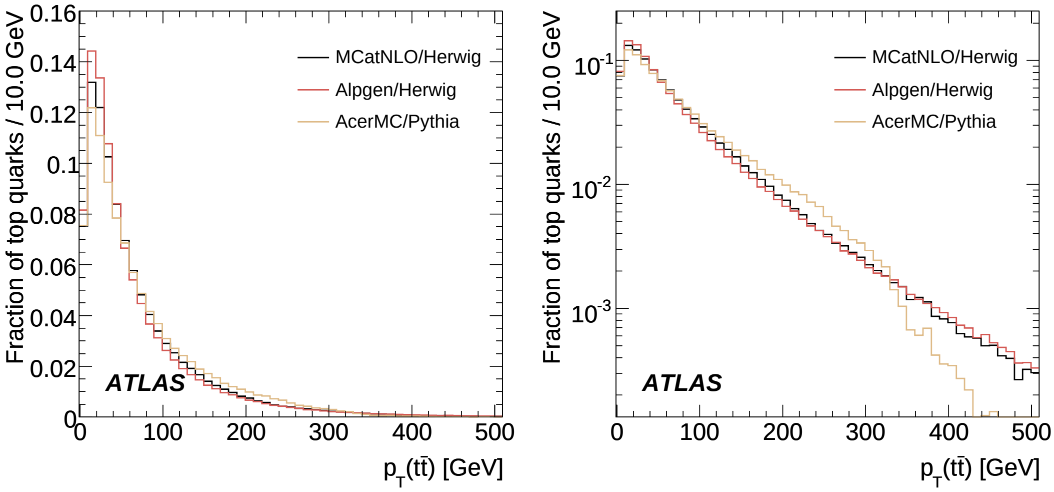

Figure 3: The transverse momentum spectrum of the $t\bar{t}$ pair on linear (left) and logarithmic scale. All distributions are normalised to unity.

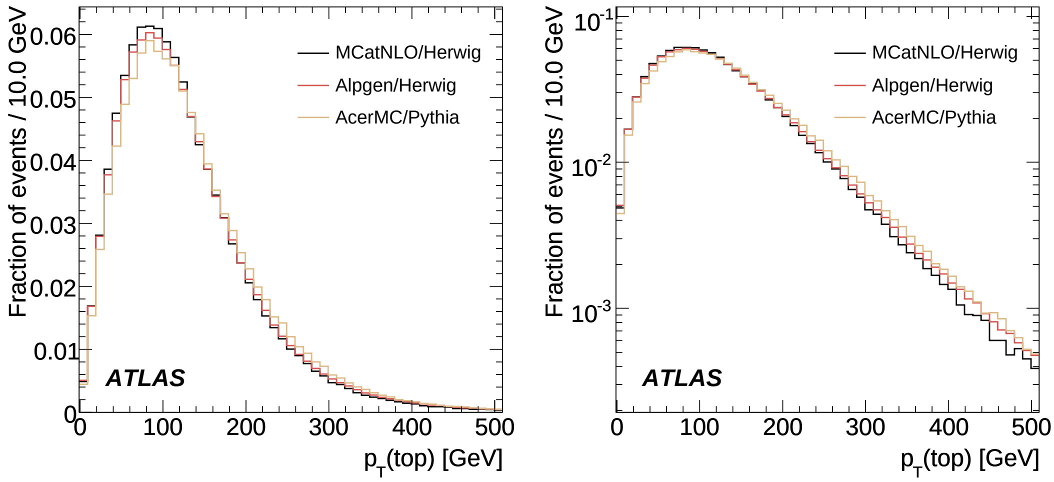

Figure 4: The transverse momentum spectrum of the top quarks on linear (left) and logarithmic scale (right). All distributions are normalised to unity.

branching ratios. The recommendation is to use the NLO values or respective k-factor in the table below. Those values have been derived in Ref. [26–28] for *s*- and *t*-channel production and in Ref. [29–31] for Wt production.

Table 5: LO and NLO cross sections for single top production in three production mechanism, *t*-channel, *s*-channel and Wt production. The values are given in pb.

channel	LO	NLO	k-factor
t- channel	251	246	0.98
s- channel	7.1	10.65	1.50
Wt	58.1	66	1.146

The uncertainty on this prediction arising from QCD scale and pdf uncertainties are: 4.0% for t-channel [29–31], 4.4% for *s*-channel [29–31] and 3% for Wt production [29–31]. An additional uncertainty arises from the not precisely known value of the mass of the top quark and has been evaluated for the *s*-channel and *t*-channel production. The uncertainty connected to the variation of the mass of the top quark by one GeV corresponds to 0.8% and 2.3% for *t*- and *s*-channel production, respectively.

5 Production of Vector Bosons in association with b quarks

5.1 $Zb\bar{b}$ production

Currently, two procedures for the production of Z bosons with *b*-quarks are pursued. In the first approach, the 2-to-3 process $gg(q\bar{q}) \rightarrow Zb\bar{b}$ is generated at LO with ACERMC, taking into account the finite mass of the *b*-quarks. No NLO calculation using massive *b*-quarks are available as today and hence the NLO is performed assuming massless b-quarks. MCFM implements NLO (and LO) calculations assuming massless b-quarks.

The effective $\sigma_{Zb\bar{b}}$ cross section has been evaluated for two different b-quark phase spaces:

- for phase space cuts of M_Z >30 GeV, $p_T^b > 10$ GeV, $|\eta_b| < 2.5$, ΔR_{bb} >0.7 and m_{bb} >9.24 GeV a k-factor of 1.424 $\pm$ 0.001 is derived (considering both gg and $q\bar{q}$ contributions). The LO cross sections (including the BR of the Z boson in electrons or muons) for the gluon and quark initiated process are $\sigma_{gg} = 52.03 \pm 0.03$ and $\sigma_{q\bar{q}} = 8.64 \pm 0.01$ pb, respectively (with a cut at 30 GeV applied on the Z boson mass). The final NLO cross section to be used for the $pp \rightarrow Zb\bar{b}$ process with the above phase space choice (optimized for the $H \rightarrow ZZ^\star \rightarrow 4l$ analysis) is:

$$\sigma_{Zb\bar{b}} = [52.03(gg) + 8.64(q\bar{q})] \text{ pb} \times 1.424 = 86.39 \text{ pb}.$$

- for phase space cuts of M_Z >60 GeV, $p_T^b > 5$ GeV, $|\eta_b| < 5$, ΔR_{bb} >0.7 and m_{bb} >9.24 GeV, a k-factor of 1.600 $\pm$ 0.005 is derived (considering both gg and $q\bar{q}$ contributions). The LO cross sections (including the BR of the Z boson muons) for the summed gluon and quark initiated process is 27.90 $\pm$ 0.04 pb (with a cut at 60 GeV applied on the Z boson mass). The final NLO cross section to be used for the $pp \rightarrow Zb\bar{b}$ process with this second phase space choice (optimized for the $A/H \rightarrow \mu\mu$ analysis) is:

$$\sigma_{Zb\bar{b}} = 27.90 \text{ pb} \times 1.600 = 44.8 \text{ pb}.$$

The uncertainty due to parton density functions corresponds to $\sim$5% while the one related to the QCD scales corresponds to $\sim$15%. All the calculations above have been obtained with CTEQ6 pdf sets.

The second approach uses SHERPA for event generation. It is based on the following matrix elements $jj \to Z$, $jj \to Zj$, $jj \to Zjj$, $jj \to Zjjj$ which are matched to the parton shower using the CKKW description. Here j denotes a parton in the initial and final states and only matrix elements with at least one j corresponding to a b (or $\bar{b}$) quark have been taken into account. The effective NLO cross section to be used for the SHERPA samples is:

$$\sigma_{Zb_{SHERPA}} = 52.3^{+5.6}_{-6.6} \text{ (stat) pb.}$$

It has been obtained by rescaling the contributions $g\bar{q} \to Zb$ and $gg(q\bar{q}) \to Zb\bar{b}$, calculated in [32] on the phase space $p_T^b > 15$ GeV, $|\eta_b| < 2.5$, by the fraction of Sherpa events fulfilling these cuts, and by the $BR(Z \to \mu\mu)$. The uncertainties due to parton density functions and choice of QCD scales has been estimated to correspond to 13%.

5.2 $Wb\bar{b}$ production

The MC used for the $Wb\bar{b}$ evgen production in the CSC notes is ALPGEN. For the NLO, two calculation are available, according to two different phase spaces, both performed using MCFM:

1. first phase space selections: $M_W > 30$ GeV, $p_T^b > 10$ GeV, $|\eta_b| < 2.5$, $\Delta R > 0.7$, $M_{bb} > 9.24$ GeV, massless b-quark. All the contributions corresponding to real emission diagrams when the additional parton is resolved as a separate jet are included in the calculation. QCD scales are set equal to the mass of the W boson. The resulting cross sections, including bothe W^+ and W^- contributions, are

   $$\sigma_{LO} = 68.7 \text{ pb - stat error} \sim 0.1\%$$
   $$\sigma_{NLO} = 176.9 \text{ pb - stat error} < 1\% \text{ - scale uncertainties} \sim 20\% \text{ - pdf uncertainties } 3.5\%$$

   resulting in a k-factor equal to 2.57 (error $< 10^{-4}$).

2. second phase space selections: no cut on W or bb masses, $|\eta(b)| < 5$, $\Delta R > 0.7$ - weak selections on leptons, all contributions corresponding to real emission diagrams when the additional parton is resolved as a separate jet are included in the calculation. The resulting k-factors (including W^+ and W^- contributions), as function of p_T are listed in Table 6.

Table 6: Differential k-factors for $Wb\bar{b}$ (W^+ and W^- contributions added), obtained from MCFM with the selection cuts explained in the text (option 2.).

p_T	k-factor
15 GeV	2.23
20 GeV	2.23
25 GeV	2.16
30 GeV	2.24
35 GeV	2.12
40 GeV	1.75

The difference between the two k-factors calculated above, O(15%), becomes almost negligible (<3-4%) once the same phase space is selected. All the calculations above have been obtained with CTEQ6 pdf sets. Uncertainty due to pdf is XXX. The recommendation for $Zb\bar{b}$ and $Wb\bar{b}$ samples is to make use of the k-factor listed above to rescale the LO ALPGEN cross sections.

The reason why $Zb\bar{b}$ ans $Wb\bar{b}$ k-factor are different is well explained in [33]. In short, it originates from the fact that the LO, the Wbb process contains only quarks in the initial state whereas the $Zb\bar{b}$ process has a gluon-gluon contribution. When the quark-gluon real emission diagrams enter at NLO they greatly enhance the $Wb\bar{b}$ cross section. Since the $Zb\bar{b}$ process is already sensitive to the gluon flux, it is not affected.

6 Multijet, charm and bottom production and minumum bias events

6.1 Inclusive jet production

The inclusive di-jet cross-section at NLO was computed with the help of the NLOJET++ package [34, 35], which is based on [36]. The di-jet cross-section obtained with this program was found to be a factor of 1.3 larger than that obtained with PYTHIA. The inclusive NLO cross section to be used for jet $P_T > 25$ GeV amounts to:

$$\sigma_{dijet} = 477 \times 10^6 \text{pb}.$$

All event samples produced with PYTHIA, HERWIG and ALPGEN should be normalised to the above cross section value for the phase space region mentioned.

6.2 Bottom and charm quark production

Inclusive production of bottom and charm quarks production were generated using PYTHIA. For the non resonant $b\bar{b}$ and $c\bar{c}$ production three different mechanisms, flavour-creation, flavour-excitation and gluon-splitting, are included in PYTHIA. The total $b\bar{b}$ or $c\bar{c}$ cross section is not well defined in PYTHIA when one includes processes other than lowest order one for $b\bar{b}$ ($c\bar{c}$) production, since PYTHIA takes the partons to be massless and therefore the cross section diverges when thw transverse momentum approaches zero. However relevant for our studies is a part of the cross section in a phase space of events passing typical trigger requiremnts for B-physics. One or two muons are required within the trigger accpetance of $|\eta| < 2.4$ and with a transverse momentum larger than 4 or 6 GeV. Table 7 summarises the predicted single and di-muon cross-sections from charm and beauty production after lepton cuts as calculated at leading order with PYTHIA5.7 using the CTEQ3L PDFs and with PYTHIA6.4 using the CTEQ6L1 PDFs. Also shown are NLO values obtained with the program FONLL [36] for some cut choices.

Table 7: Cross sections for $b\bar{b}$ and $c\bar{c}$ production after various muon and di-muon requirements.

Process	PYTHIA6.4	PYTHIA5.7	FONLL
$b\bar{b} \rightarrow \mu 6X$	6.1 μb	2.4 μb	2.8+0.9-0.5μb
$b\bar{b} \rightarrow \mu 4X$	19.3 μb		
$c\bar{c} \rightarrow \mu 6X$	7.9 μb	1.1 μb	2.9++0.9-0.5μb
$c\bar{c} \rightarrow \mu 4X$	26.3 μb		
$b\bar{b} \rightarrow \mu 6\mu 4X$	110.5 nb		
$b\bar{b} \rightarrow \mu 4\mu 4X$	212.0 nb		
$c\bar{c} \rightarrow \mu 6\mu 4X$	248.0 nb		
$c\bar{c} \rightarrow \mu 4\mu 4X$	386.0 nb		

The values quoted have large theoretical uncertainties from missing higher order corrections. The recommendation is to use an uncertainty range corresponding to the difference observed when comparing the two different PYTHIA versions. Compared to this the uncertainty arising from variations of the PDFs is relatively small and amounts to approximately 20%.

6.3 Minimum bias events

Proton-proton interactons can be divided into elastic and inelastic components, and the inelastic component can be further divided into: non-diffractive, single diffractive and double diffractive components [37, 38]. The total cross-section (σ_{tot}) can thus be written as:

$$\sigma_{tot} = \sigma_{elas} + \sigma_{sd} + \sigma_{dd} + \sigma_{nd}$$

where these cross-sections are elastic (σ_{elas}), single diffractive (σ_{sd}), double diffractive (σ_{dd}) and non-diffractive (σ_{nd}), respectively. The cross-sections for the inelastic subprocesses determined using PYTHIA are given in Table 8. Some models for hadronic interactions, such as PHOJET [39, 40], also include central diffraction as a component of the inelastic cross-section. Central diffraction typically contributes at the per-cent level to the total cross-section. PHOJET predictions for inelastic cross-sections are also shown in Table 8.

The acceptance of inelastic events is defined by the trigger, which is usually known as a minimum bias trigger. It is so named because it is designed to avoid bias in the sample, such as selecting high-p_T events by triggering on high-p_T objects. However, some bias is usually introduced due to effects such as the geometrical acceptance of the trigger or minimum energy thresholds in the trigger. It is therefore not unusual to find slightly different definitions for minimum bias events in the literature. Historically, the minimum bias triggering systems used in hadron collider experiments favoured the detection of non-single diffractive (NSD) inelastic events, i.e. $\sigma_{minimum\ bias} = \sigma_{nsd} = \sigma_{tot} - \sigma_{elas} - \sigma_{sd}$. This selection is particularly characteristic of experiments employing two-arm coincidence hits as a minimum bias trigger which suppresses the single-diffractive events. Non-single diffractive events have thus been customarily classified as 'minimum bias events'. The minimum bias trigger typically accepts events in the central region of an experiment and therefore does not include elastic scattering.

It is recommended to use the PYTHIA values in Tab 8 as central cross section values for the analysis. The difference between the PHOJET and PYTHIA values might be considered as a rough first estimate of the uncertainty associated with those numbers. Variations of the PDF in the PYTHIA model do not change the findings for the total, elastic and inelastic cross sections. Only the relative contributions of single-, double- and non-diffractive processes is modified by the variation of the PDFs.

Table 8: Cross-section predictions for p-p collisions at $\sqrt{s} = 14$TeV from PYTHIA evaluated with CTE5L PDF and PHOJET evaluated with GRV94 PDF.

	Cross section (mb)	
Process	PHOJET	PYTHIA
non-diff.	68.7	54.7
single diff.	10.8	14.3
double diff.	4.1	10.2
central diff.	1.0	-
total inelastic	84.6	79.2
elastic	34.5	22.5
total	119.1	101.7

References

[1] Pumplin, J. and others, JHEP **07** (2002) 012.

[2] Stump, Daniel and others, JHEP **10** (2003) 046.

[3] Tung, W. K. and others, JHEP **02** (2007) 053.

[4] Pumplin, J. and Belyaev, A. and Huston, J. and Stump, D. and Tung, W. K., JHEP **02** (2006) 032.

[5] Sjostrand, Torbjorn and Mrenna, Stephen and Skands, Peter, JHEP **05** (2006) 026.

[6] Corcella, G. and others, HERWIG 6.5 release note, 2002, hep-ph/0011363,hep-ph/0210213.

[7] Moretti, Stefano, HERWIG: An event generator for e+ e- linear colliders, 2002, hep-ph/0209209.

[8] Corcella, G. and others, JHEP **01** (2001) 010.

[9] Mangano, Michelangelo L. and Moretti, Mauro and Piccinini, Fulvio and Pittau, Roberto and Polosa, Antonio D., JHEP **07** (2003) 001.

[10] Caravaglios, F. and Mangano, Michelangelo L. and Moretti, M. and Pittau, R., Nucl. Phys. **B539** (1999) 215–232.

[11] Mangano, Michelangelo L. and Moretti, Mauro and Pittau, Roberto, Nucl. Phys. **B632** (2002) 343–362.

[12] Gleisberg, Tanju and others, JHEP **02** (2004) 056.

[13] Hoche, Stefan and others, Matching parton showers and matrix elements, 2006, hep-ph/0602031.

[14] Melnikov, Kirill and Petriello, Frank, Phys. Rev. Lett. **96** (2006) 231803.

[15] Melnikov, Kirill and Petriello, Frank, Phys. Rev. **D74** (2006) 114017.

[16] C. Balazs, E. Berger, S. Mrenna and C.-P. Yuan, Phys. Rev. **D57** (1998) 6934.

[17] C. Balazs, E. Berger, P. Nadolsky, C. Schmidt and C.-P. Yuan, Phys. Lett. **B489** (2000) 157.

[18] C. Balazs, E. Berger, P. Nadolsky and C.-P. Yuan, Phys. Lett. **B637** (2006) 235.

[19] S. Catani, M. Fontannaz, J.P. Guillet, and E. Pilon, JHEP **05** (2002) 028.

[20] N.E. Adam et al., Higgs Working Group Summary Report, 2008, arXiv:0803.1154 [Unknown].

[21] T. Binoth *et al.*, E. Phys. J. **C16** (2000) 311.

[22] M. Escalier, et al., Search for a Standard Model Higgs Boson with the ATLAS Experiment in the $H \to \gamma\gamma$ Channel, ATLAS Internal Note ATL-PHYS-INT-2006-002(2006).

[23] Kidonakis, Nikolaos and Vogt, Ramona, Phys. Rev. **D68** (2003) 114014.

[24] Bonciani, Roberto, Catani, Stefano and Mangano, Michelangelo L. and Nason, Paolo, Nucl. Phys. **B529** (1998) 424–450.

[25] Kersevan, Borut Paul and Richter-Was, Elzbieta, The Monte Carlo event generator AcerMC version 2.0 with interfaces to PYTHIA 6.2 and HERWIG 6.5, 2004, hep-ph/0405247.

[26] Sullivan, Zack, Phys. Rev. **D70** (2004) 114012.

[27] Cao, Qing-Hong and Schwienhorst, Reinhard and Benitez, Jorge A. and Brock, Raymond and Yuan, C. -P., Phys. Rev. **D72** (2005) 094027.

[28] Cao, Qing-Hong and Schwienhorst, Reinhard and Yuan, C. -P., Phys. Rev. **D71** (2005) 054023.

[29] Belyaev, A. and Boos, E., Phys. Rev. **D63** (2001) 034012.

[30] Tait, Tim M. P., Phys. Rev. **D61** (2000) 034001.

[31] Campbell, John and Tramontano, Francesco, Nucl. Phys. **B726** (2005) 109–130.

[32] Campbell, J. and Ellis, R. Keith and Maltoni, F. and Willenbrock, S., Phys. Rev. **D69** (2004) 074021.

[33] Campbell, John and Ellis, R. Keith and Rainwater, David L., Phys. Rev. **D68** (2003) 094021.

[34] Z. Nagy, Phys. Rev. Lett. **88** (2002) 122003.

[35] Z. Nagy, Phys. Rev. **D68** (2003) 094002.

[36] S. Catani and M.H. Seymour, Nucl. Phys. **B485** (1997) 291–419.

[37] Block, M. and Fletcher, R. and Halzen, F. and Margolis, B. and Valin, P., Phys. Rev. **D41** (1990) 978.

[38] Block, M. M. and Halzen, F. and Margolis, B., Phys. Lett. **B252** (1990) 481–482.

[39] Engel, R. and Ranft, J. and Roesler, S., Phys. Rev. **D55** (1997) 6957–6967.

[40] Engel, R., Z. Phys. **C66** (1995) 203–214.